Heliyon 5 (2019) e02765

Contents lists available at ScienceDirect

Heliyon

journal homepage: www.heliyon.com

Heliyon

Research article

Antibacterial efficacy of green synthesized α-Fe_2O_3 nanoparticles using *Sida cordifolia* plant extract

Panduranga Naga Vijay Kumar Pallela [a], Shameem Ummey [b], Lakshmi Kalyani Ruddaraju [c], Satyananarayana Gadi [a], Chinmai SailajaLakshmi Cherukuri [a], Sailaja Barla [a], S.V.N. Pammi [d,*]

[a] *Advanced Analytical Laboratory, Andhra University, Visakhapatnam, 530003, India*
[b] *Department of Zoology, Andhra University, Visakhapatnam, 530003, India*
[c] *Shri Vishnu College of Pharmacy, Bhimavaram, Andhra Pradhesh, 530041, India*
[d] *Department of Materials Science and Engineering, Chungnam National University, Daeduk Science Town, Daejeon, 305-764, Republic of Korea*

ARTICLE INFO

Keywords:
Biotechnology
Microbiology
Nanotechnology
Nanomaterials
Materials property
Materials synthesis
Secondary metabolites
Green synthesis
Iron oxide
Antibacterial activity
S. cordifolia

ABSTRACT

The aim of the work is to synthesize iron oxide (α-Fe_2O_3) nanoparticles using *Sida cordifolia* plant extract along with evaluation of its antibacterial activity. The presence of phytochemicals in *Sida cordifolia* methanolic plant extract was investigated by HPTLC and LC-MS/TOF. The probable mechanism for formation of α-Fe_2O_3 nanoparticles in mediation with plant extract was demonstrated. The green synthesized iron oxide nanoparticles (α-Fe_2O_3 NPs) were characterized by using X-ray diffraction, scanning, and transmission electronic microscopy, TG-DTA, FTIR, and UV spectroscopy. The crystallite size of prepared α-Fe_2O_3 nanoparticles estimated via Debye-Scherrer formula and Williamson-Hall plot was around 20 nm which is in accordance with particle size in TEM images. The *S. cordifolia* mediated iron-oxide nanoparticles (α-Fe_2O_3 NPs) hold potent antibacterial activity against various gram positive and gram negative bacteria.

1. Introduction

Recent years have eye-witnessed an extensive study of magnetic nanoparticles (α-Fe_2O_3, γ-Fe_2O_3, Fe_3O_4 and FeO) for diverse fundamental and biomedical applications [1, 2, 3, 4, 5]. Among different polymorphs of iron oxide, hematite (α-Fe_2O_3) is more stable with anti-corrosive properties, tuneable optical and magnetic properties, excellent chemical stability and biocompatibility with inexpensiveness that provide applicability in various technological applications. These advantages of hematite accommodated innovative nano inventions for applications in catalysts, high-density magnetic storage media, anticorrosive agents, pigments, water splitting, water purification, solar energy conversion and gas sensors [6, 7, 8]. Besides these, α-Fe_2O_3 nanoparticles are more suitable for biomedical applications due to their high chemical stability and less toxicity with biocompatibility [9].

Many approaches have been reported for iron nanoparticles syntheses via chemical routes that involves usage of toxic solvents, which could possibly create hazardous byproducts, and physical methods that usually require high energy and vacuum. These drawbacks enable awareness for the necessity to synthesize NPs in a safe, environment-friendly procedure in a more economical way [10]. From the past decade, utilizing biological systems to synthesize metallic and metal oxide nanoparticles have been greatly explored. Our previous studies also focused on plant and their parts (leaves and roots) extract mediated preparation of metallic and metal oxide NPs [11, 12, 13, 14]. Recently there are reports on the plant-mediated synthesis of iron oxide nanoparticles. However, very few reports are available with hematite phase, which were reported with non-uniformity and large deviation in particle size and none of these reports elucidated the antibacterial activity of iron oxide nanoparticles [15, 16, 17, 18, 19].

The major medicinal benefits of the *Sida cordifolia* plant extract has been demonstrated in our recent study [11]. Herein, we carried out green synthesis of α-Fe_2O_3 NPs from the solution of iron nitrate using *Sida cordifolia* plant extract as a reducing agent without using any surfactant. In addition, we also examined the possible potent compounds presented in *Sida cordifolia* plant extract via (HPTLC and LC-MS/TOF) that might be responsible for the reduction of iron nitrate into α-Fe_2O_3 NPs and for stabilization of α-Fe_2O_3 NPs. The advantage of employing *Sida cordifolia*

* Corresponding author.
E-mail address: sreepammi@gmail.com (S.V.N. Pammi).

https://doi.org/10.1016/j.heliyon.2019.e02765
Received 28 November 2018; Received in revised form 18 July 2019; Accepted 30 October 2019

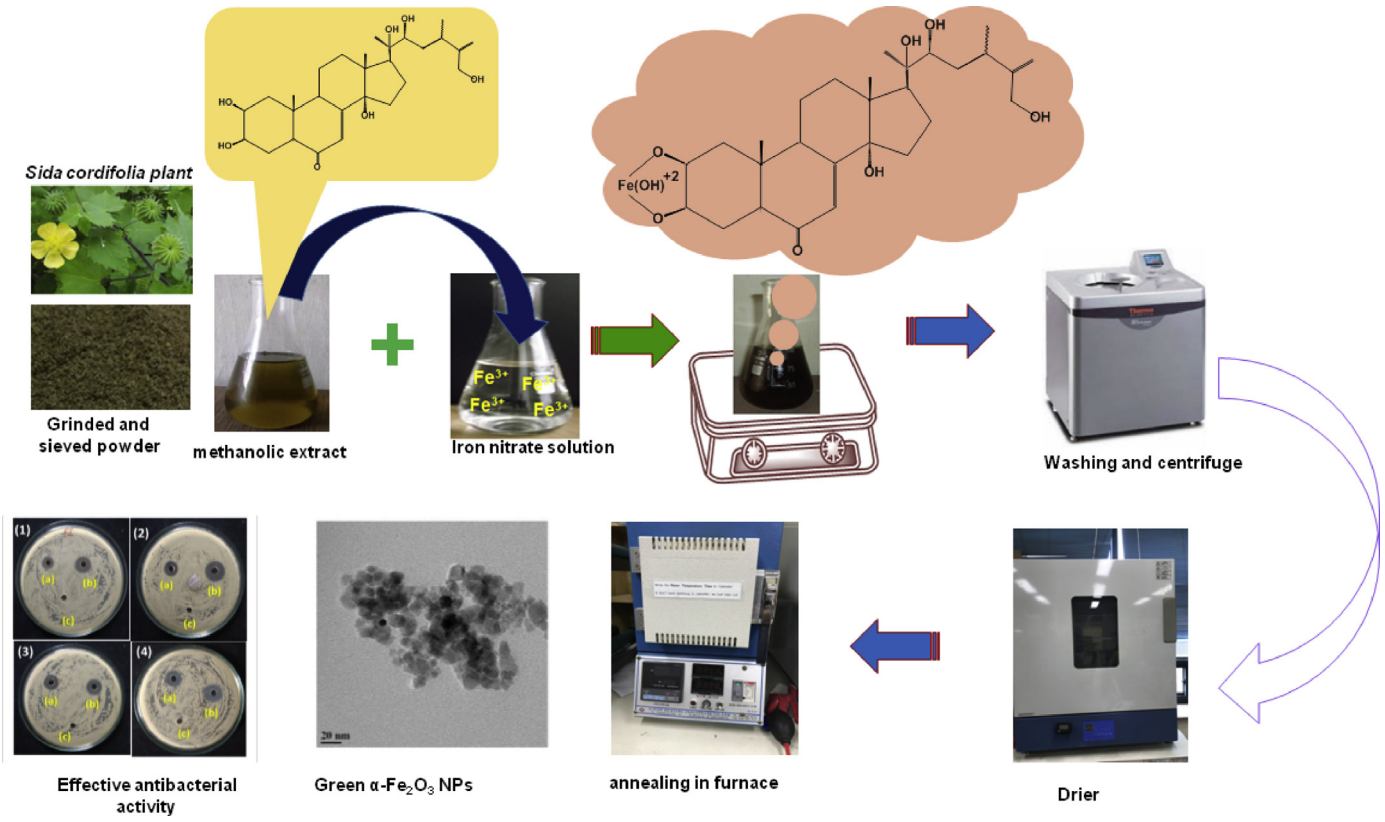

Fig. 1. Schematic illustration of the present study with plausible formation-mechanism of α-Fe_2O_3 nanoparticles.

plant than other plants or other green synthetic methods (microbial based) is controlled synthesis of nanoparticles due to wide range of phytochemicals associated in the whole plant and to avoid complexity associated with microbial synthesis respectively.

The antimicrobial activity of α-Fe_2O_3 NPs was tested against *E. coli*, *K. pneumoniae*, *B. subtilis*, and *S. aureus*. The problems associated with conventional methods (the use of toxic stabilizers, solvents, and surfactants) encouraged to synthesize biocompatible α-Fe_2O_3 NPs

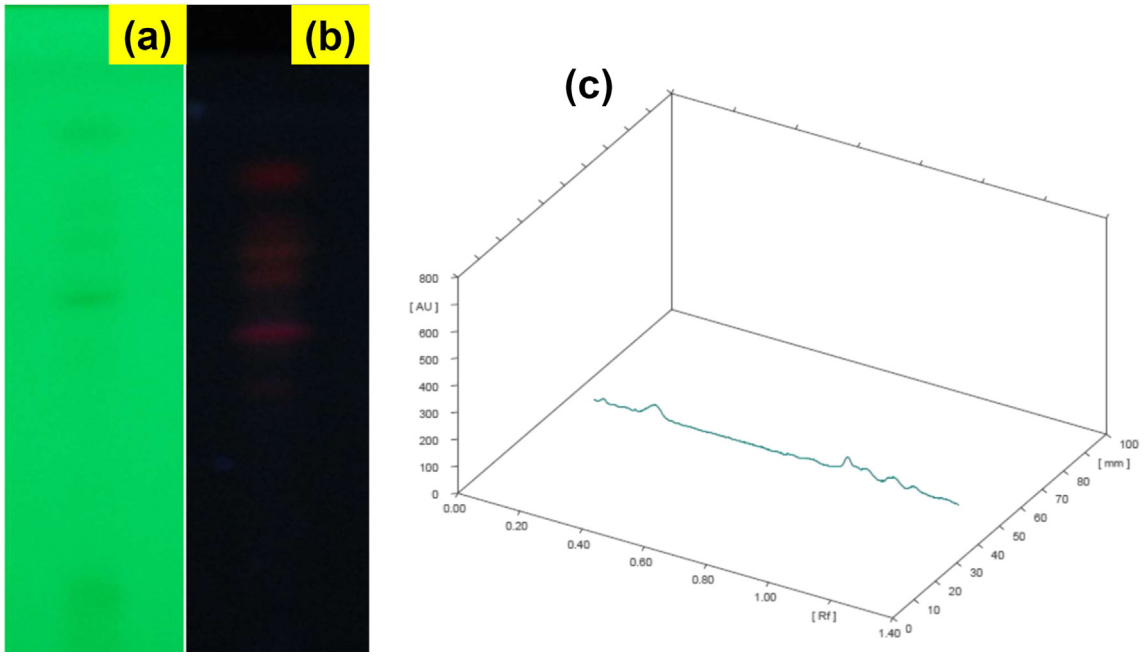

Fig. 2. TLC plate image of methanolic extract of *S. cordifolia Plant* at 254 nm (a) 366 nm (b) and (c) HPTLC Chromatographic profile (3D) of *S. cordifolia* plant methonalic extract.

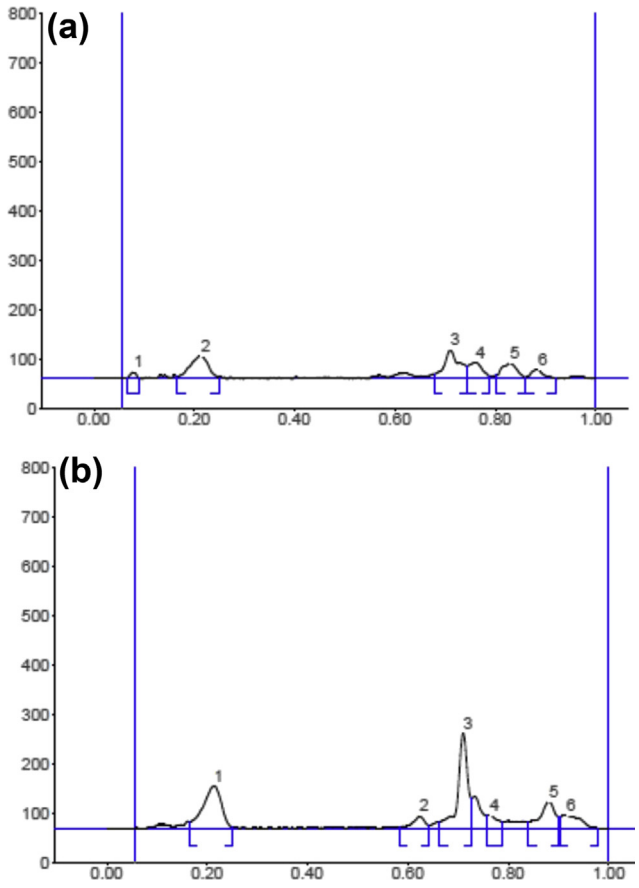

Fig. 3. Finger printing analysis of *S. cordifolia* plant methonalic extract at 254 nm (a) and 366 nm (b).

nanoparticles using *Sida cordifolia* plant extract as an effective stabilizing agent and capping agent, which might also impart synergetic antibacterial potency due to rich source of metabolites with medicinal properties. The iron oxide nanoparticles were tested for antibacterial activity in consideration with resistant development to all the known classes of antibiotics [10]. This is the ever first report to elucidate the phytochemicals in *Sida cordifolia* plant extract and to synthesize *Sida cordifolia* extract mediated α -Fe_2O_3 NPs that proves its antibacterial efficacy. The schematic representation of the present study is clearly depicts in Fig. 1.

2. Materials and methods

2.1. Materials

Sida cordifolia herbal plant was collected from the local area of University campus, authenticated and deposited in the Botany department herbarium (B.D.H), with voucher number AU (B.D.H)-22082. The test organisms selected include both gram-positive bacteria i.e., *Bacillus subtilis* (NCIM 2063), *Staphylococcus aureus* (NCIM 2079) and gram-negative bacteria i.e., *Escherichia coli* (2065), *Klebsiella pneumonia* (NCIM 2327) and were obtained from National Collection of Industrial Microorganisms (NCIM).

2.2. Preparation of S. cordifolia extract

S. cordifolia plant was thoroughly washed thrice with tap water and dried in shade. Dried plants were cut into small pieces and ground coarsely using pulverizer. The coarse powder was extracted using methanol in the Soxhlet apparatus. The obtained crude extract was concentrated under reduced pressure and was refrigerated for further use.

2.3. Phytochemical identification in methanolic extract of S. cordifolia by HPTLC and LC-MS/TOF

Plant extract was subjected to the chemical tests using standard procedures for screening of phytochemicals and phytochemicals were confirmed by the HPTLC and LC-MS/TOF. HPTLC fingerprint analysis was carried out on the methanolic extract of *S. cordifolia* (10 μL). The extract was applied on 10 cm × 10 cm aluminum backed HPTLC plates coated with silica gel (60 F 254) of 0.25 mm layer thickness. CAMAG HPTLC system consists of Linomat v spotting and scanner 3 with the mobile phase i.e. Toluene: Chloroform: Ethanol (2.6: 6: 1.4). The chromatogram obtained was studied under 254 nm, 366 nm.

The LC-MS/TOF system consisted of Agilent LC-MS/TOF (6200 series TOF/6500 series Q-TOF B.08.00). LC analyses was performed on a C18 column (Agilent) at a column temperature of 25 °C. A volume of 10 μL of sample was injected using auto sampler. The mobile phase consisted of MilliQ water (solvent A) and acetonitrile (solvent B). The flow rate was set at 500 μL/min. The column was equilibrated (A: B; v/v) in 90:10 (5 min), and elution was carried out using the following steps; 90:10 (5 min), 80:20 (5 min), 70:30 (5 min), 60:40 (5 min), 50:50 (5 min), a linear gradient increase from 50% B to 100% (5 min), and 100% B (7 min).

2.4. Synthesis of iron oxide nanoparticles

In a typical experiment, a 0.01 M precursor solution of iron nitrate was prepared with double-distilled water and stirred well using magnetic stirrer for 30 min. Freshly prepared *S. cordifolia* extract was used as a reducing agent and stabilizer. For the green synthesis of iron oxide nanoparticles, the aqueous precursor solution was kept under uniform stirring and boiled at 60 °C for 5 min. 5mL of *S. cordifolia* extract was added to 10 mL of boiled precursor solution under continuous stirring. The precursor solution turns deep brown and precipitate was formed after addition of *S. cordifolia* extract. To ensure homogeneous reaction, this process has been done under continuous stirring. The collected precipitate solution was centrifuged at 10000 rpm for 10 min with acetone, ethanol and DI water repeatedly. The dried precipitate powder was annealed at 300 °C for 8 h to obtain deep red colored α-Fe_2O_3 nanoparticles.

2.5. Characterization of iron oxide nanoparticles

The morphological, structural, chemical composition of nanoparticles were analyzed with SEM–EDX (JEOL JSM-6610-LV- with Oxford EDS), XRD (PANalytical: XPERT-PRO) Thermal analyses of the samples were done using TG-DTA (STA7300- HITACHI) and functional groups were identified by FTIR (Shimadzu FT-IR 21) Prestige equipment and UV-VIS (Shimadzu UV-VIS 2450) spectral analysis was performed to analyze the characteristic peaks.

2.6. Antibacterial effect of iron oxide nanoparticles

Agar well diffusion method was employed to determine the antimicrobial activity of the synthesized *Sida cordifolia* mediated iron oxide

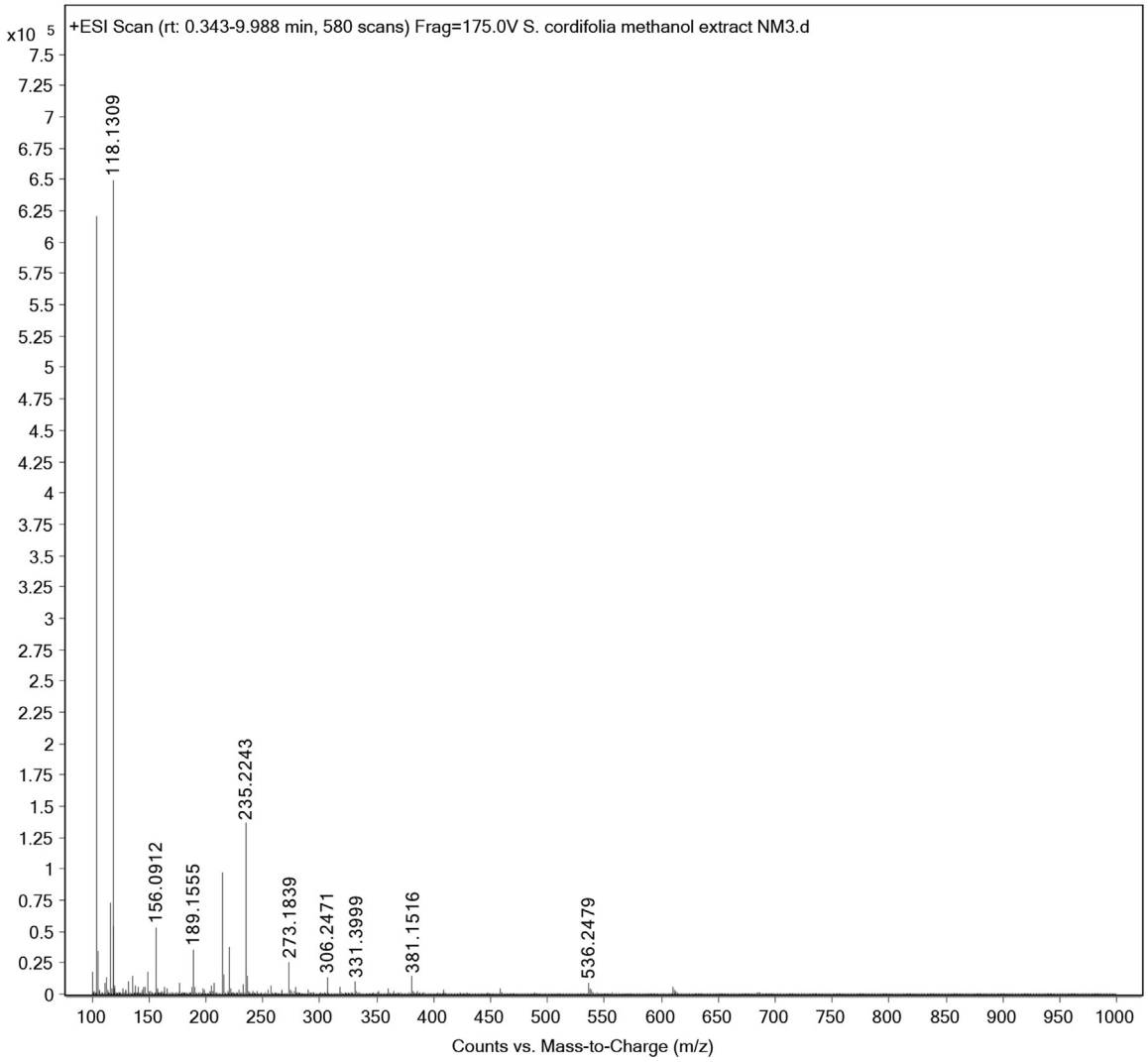

Fig. 4. *S. cordifolia* extract LC-MS/TOF masses of different compounds.

nanoparticles (SCINP). Strains viz., *Bacillus subtilis* (NCIM-2063), *Staphylococcus aureus* (NCIM-2079), *Escherichia coli* (NCIM- 2065), and *Klebsiella pneumonia* (NCIM-2327) were used to assess the antibacterial activity of synthesized nanoparticles. Muller Hinton agar plates were prepared and swabbed with the broth culture of the respective bacteria. Three wells were bored in each plate with a sterile cork borer. Stock solutions of SCINPs, neomycin (control) were prepared at a concentration of 1 mg/ml in distilled water and plant extract was used as a negative control. 50 μL of these samples were added to each well. The plates were incubated at 37 °C for 24 h.

3. Results and discussion

The initial phytochemical examination was carried out on *S. cordifolia* methanolic extract, which displayed the presence of various phytoconstituents including alkaloids, carbohydrates, glycosides, proteins, tannins, flavonoids and terpenoids by various reagent tests. These results were confirmed from different spots on HPTLC silica plate running with mobile phase at 254 nm and 366 nm (Fig. 2a and b). Fingerprint analysis was carried out on the methanolic extract of *S. cordifolia* using CAMAG HPTLC system. HPTLC Chromatographic profile (3D) of *S. cordifolia* plant methonalic extract has been provided in Fig. 2c. The fingerprint R_f value of different compounds at 254 nm illustrated six spots at 0.08, 0.21, 0.84, 0.93, 1.00, 1.07. The R_f value of different compounds at 366 nm as six spots are noticed at 0.20, 0.73, 0.83, 0.94, 1.05, 1.12 (Fig. 3a and b). This reveals that various phytochemical constituents are present in the methanolic extract of *S. cordifolia.*

LC-MS/TOF (time of flight) analysis of the *S. cordifolia* extract confirmed the presence of various compounds with different molecular mass showing 40 min retention time (RT). The LCMS/TOF scan exhibited distinct RTs for the compounds present in the extract samples as shown in Fig. 3.

The possible mechanism of formation of α-Fe_2O_3 nanoparticles using *Sida cordifolia* plant extract has been provided with schematic representation in Fig. 4. Initially, octahedral aqua complex of Fe(III), $Fe(H_2O)_6$ is formed instantaneously in water, which decomposes into $Fe(OH)^{2+}$ via deprotonation of coordinated water molecule [20]. The hydrolysed iron species could form a complex with the functional groups in glycosides, flavonoids, phenols which are rich source in *sida cordifolia* plant extract [21]. With the increase in the temperature, a phase transformation of iron species into Fe $(OH)^{2+}$ might occur that eventually form primary particles (Fe_2O_3) with nano scale. These primary particles have high

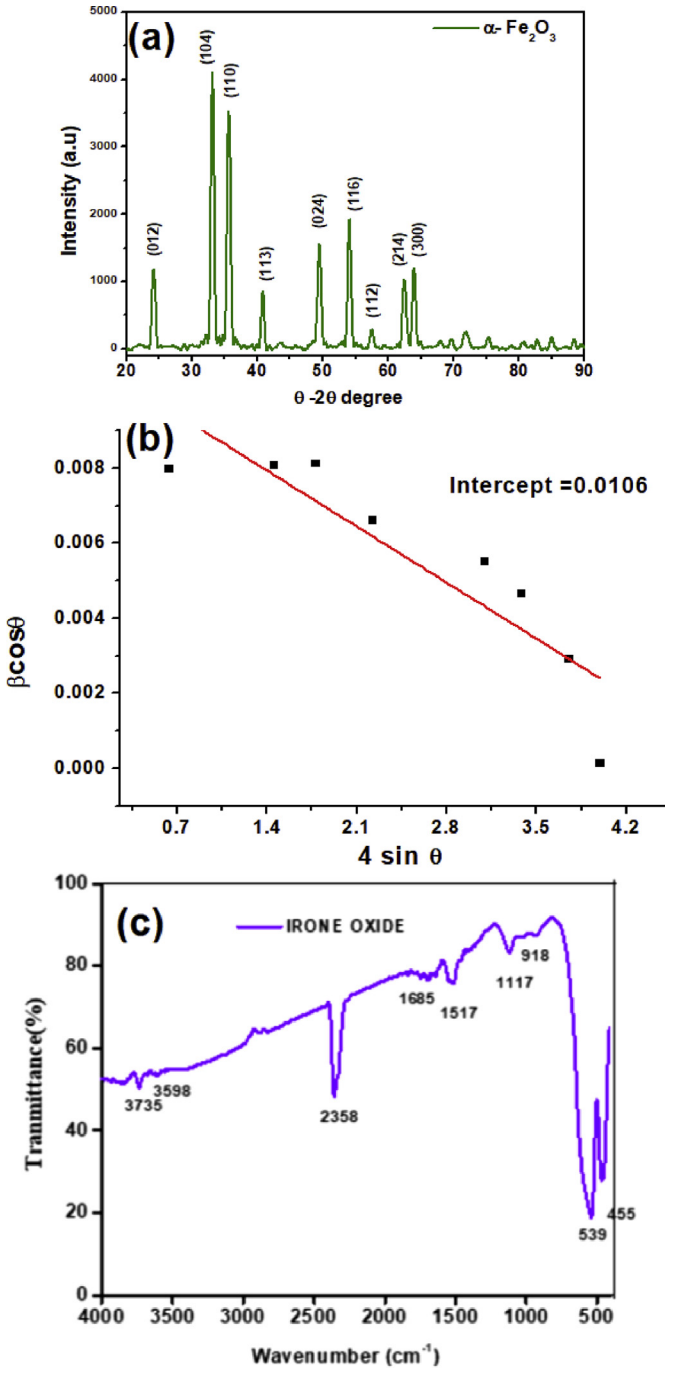

Fig. 5. (a). XRD pattern (b) Williamson-Hall plot of β_{tot} cos θ against C sin θ (where C = 4) calculated from XRD spectra and (c) FTIR analysis of green synthesis of *S. cordifolia* mediated α-Fe_2O_3 nanoparticles.

surface energy and aggregate quickly to minimize their surface energy [22].

XRD pattern of *S. cordifolia* extract mediated iron oxide NPs revealed the diffraction peaks at 24.20°, 33.19°, 35.68°, 40.87°, 49.52°, 54.10°, and 64.00°, respectively indexed to (012), (104), (110), (113), (440), (024), (116) and (300) planes of the rhombohedral hematite phase of magnetite nanoparticles (α-Fe_2O_3) (JCPDS 89-0599) (Fig. 5a). There is no trace of additional planes observed from XRD pattern, which indicates that the green synthesized α-Fe_2O_3 NPs were obtained with high purity at low temperatures. The calculated crystallite size calculated via Debye-Scherrer formula for predominant plane (104) of green synthesized hematite nanoparticles was about 18 nm. Further, we have calculated the crystallite size using Williamson-Hall plot (Fig. 5b) and was about 15nm [23].

FTIR analysis was performed to identify the presence of phytochemicals on the surface of the α-Fe_2O_3 nanoparticles. The results were recorded to identify the functional groups of the phytoconstituents responsible for the reduction and stabilizing the α-Fe_2O_3 nanoparticles. Fig. 5c shows the IR spectra of α-Fe_2O_3 nanoparticles recorded in between 400-4000 cm^{-1}. The presence of magnetite nanoparticles can be confirmed by the strong peaks around 455 cm^{-1} and 539 cm^{-1} corresponding to Fe–O stretches of α-Fe_2O_3 [23]. The other peaks at 918 cm^{-1}, 1117 cm^{-1} corresponds to C–O stretches, 1517 cm^{-1} to N=O stretches, 2353 cm^{-1} and 3735 cm^{-1} stretches assigns to O–*H group*, which are assumed to be the phytoconstituents that are responsible for reduction of metal ions from precursor and capping of α-Fe_2O_3 nanoparticles [11].

The surface morphology of the green synthesized iron oxide nanoparticles was analyzed initially by scanning electron microscopy (SEM). As shown in Fig. 6a, the SEM images of the α-Fe_2O_3 have shown the formation of spherical nano clusters, which contain a large number of smaller nanoparticles that are attributed from the aggregation of the nanoparticles. The elemental composition of the synthesized nanoparticles was evaluated by EDS analysis. The result indicated that the nanoparticles hold about 39.37% of iron and 60.63% of oxygen (Fig. 6b), which indicated the purity of the formed hematite phase of nanoparticles. For further confirmation of size and morphology of the green synthesized iron oxide nanoparticles, TEM analysis has been done and is shown in Fig. 6c and d. The TEM images revealed asymmetric morphology with uniform dispersion during formation of hematite phase. The particle size of hematite nanoparticles was 10–22 nm with an average size of 16 nm, which was predicted from XRD analysis using Debye-Scherrer formula and Williamson-Hall plot. The measured interplanar spacing distance was 0.27 nm. HRTEM image (Fig. 6d) found to be in match with (104) plane of hematite phase.

TG & DTA analysis of green synthesized Fe_2O_3 nanoparticles is shown in Fig. 7. The temperature range of measure is 30 °C–800 °C. In the TG analysis, the total weight loss percentage in the sample is 13.6%. The initial weight loss of 12.5% was observed below 400 °C corresponding to loss of superficial water molecules and the phytoconstituents on the surface of the nanoparticles. The temperature range of 400–800 °C displayed the weight loss of only about 1.1%. This corresponds to phase transformation from mixed phases of iron oxides into α-Fe_2O_3 phase [9, 23] It is interesting to note that the less amount of weight loss is between 400- 800 °C indicating complete formation of α-Fe_2O_3 phase during synthesis. From DTA, one exothermic and one endothermic peak were detected. Both the endothermic and exothermic peaks were observed due to phase transformation. It corresponds to the complete liberation of carbonaceous and other inorganic materials in the sample and it infers that the sample has biological plant extract and thus, more weight loss [23, 24].

Antibacterial activity of green synthesized α-Fe_2O_3 nanoparticles (50 μg/ml) and the commercial antibiotic (50 μg/ml) have been examined and significant Zone of inhibitions (ZOI) were observed as shown in Fig. 7. In the present study, we have tested the antibacterial activity of α-Fe_2O_3 NPs was performed against *B. subtilis*, *S. aureus*, *E. coli,* and *K. pneumonia* using the agar well-diffusion method. From the values of ZOI, α-Fe_2O_3 NPs are more efficient to inhibit the growth of *B. subtilis*, as the maximum zone of inhibition (ZOI) was 16.00 ± 1.00 mm has been observed. The zone of inhibition of green synthesized α-Fe_2O_3 NPs against *S. aureus*, *E. coli*, and *K. pneumonia* were 13.67 ± 0.58, 11.33 ± 0.58 and 12.00 ± 1.00 mm respectively. From reported literature,

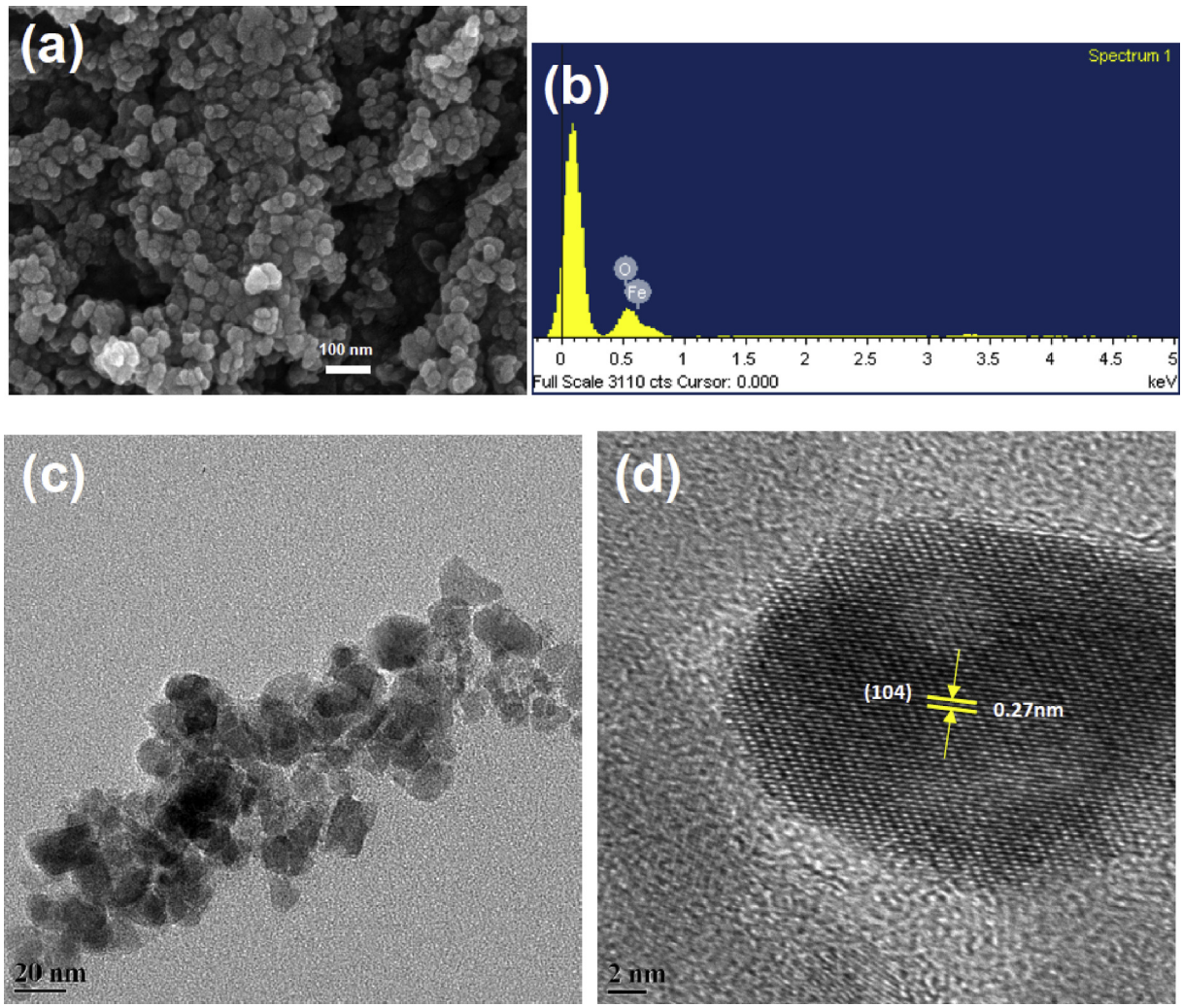

Fig. 6. (a) SEM, (b) EDS, (c) TEM and (d) HRTEM analysis of green synthesis of *S. cordifolia* mediated α-Fe_2O_3 nanoparticles.

hematite NPs (α-Fe_2O_3) are more efficient against Gram-positive bacterial strain than the Gram-negative which is similar to present study. These results were compared to commercial antibiotic neomycin and the zone of inhibition was 17.00, 15.00, 15.00 and 19.00, mm for *B. subtilis*, *S. aureus*, *E. coli,* and *K. pneumonia* respectively (Fig. 7b). There are two possible mechanisms demonstrated for hematite (α-Fe_2O_3) NPs against Gram positive or Gram-negative bacteria. As these α-Fe_2O_3 NPs are highly stable in ambient environment there is less contribution of metal ion release for antibacterial activity. In contrast, UV activates production of reactive oxygen species from the defect sites of α-Fe_2O_3 or visible light electron-hole pairs are created. The created electron hole pairs can contribute to generation of reactive oxygen species such as superoxide radical anions ($O2^-$), hydroxyl radicals (OH^-) etc. The generated free radicals O_2^- and OH^- can desorption of membrane leading to death of the bacteria [24]. In addition, different interactions like electrostatic, dipole-dipole, hydrogen bond, hydrophobic and van der wall's interactions are responsible for disruption of cellular function and disruption and disorganization of membranes [23].

4. Conclusion

The green fabrication of iron oxide nanoparticles was carried out using *S. cordifolia* extract. The extract contains a rich source of phytochemicals as proved from HPTLC and LC-MS/TOF results and is found to be very effective reducing and stabilizing agent for formation of SCINP. *S. cordifolia* mediated iron oxide nanoparticles serves as potent antibacterial agents in an eco-friendly way by securing natural microbiome as nanoparticles usually acts through targeted delivery. Thus, *S. cordifolia* mediated iron oxide nanoparticles can act as an alternative antimicrobial agent to the prevailing antibiotics.

Declarations

Author contribution statement

P.P.N. Vijay Kumar: Conceived and designed the experiments; Performed the experiments.

U. Shameem: Conceived and designed the experiments; Contributed reagents, materials, analysis tools or data.

G. Satyananarayana: Performed the experiments; Contributed reagents, materials, analysis tools or data.

Sailaja lakshmi Ch.C. & B. Sailaja: Performed the experiments; Analyzed and interpreted the data.

S.V.N. Pammi: Conceived and designed the experiments; Analyzed and interpreted the data; Contributed reagents, materials, analysis tools or data; Wrote the paper.

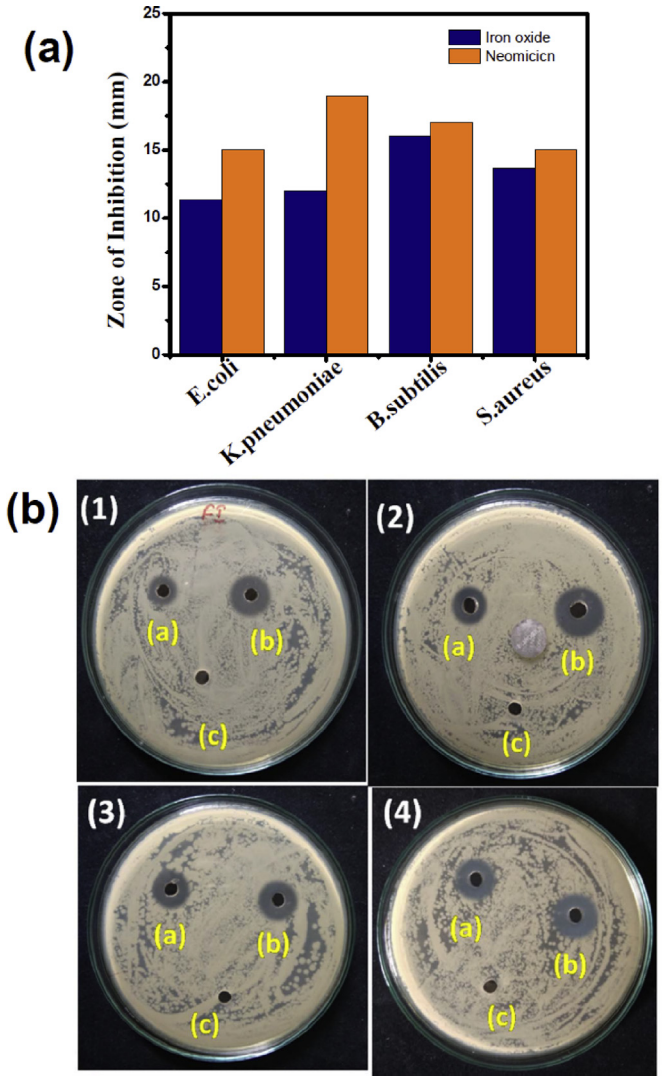

Fig. 7. (a) comparison of Zone of inhibition for green synthesis of *S. cordifolia* mediated α-Fe_2O_3 nanoparticles and standard antibiotic with 50 μg/ml against tested bacteria (b) Zone of inhibition of (a) α-Fe_2O_3 (50 μg/mL) (b) standard antibiotic (50 μg/mL) and (c) Plant extract against (1) *E. coli*, (2) *K. pneumonia*, (3) *B. subtilis* (4) *S. aureus* bacterial pathogens.

R.L. Kalyani: Analyzed and interpreted the data; Wrote the paper.

Funding statement

This work was supported by the DST-PURSE Programme.

Competing interest statement

The authors declare no conflict of interest.

Additional information

No additional information is available for this paper.

Acknowledgements

We are thankful to the DST-PURSE Programme, Advanced Analytical Laboratory, Andhra University for their support in carrying out in this research work regarding SEM-EDX and XRD, TG-DTA, FTIR and UV spectroscopy analysis.

References

[1] M.S. Akhtar, J. Panwar, Y.S. Yun, Biogenic synthesis of metallic nanoparticles by plant extracts, ACS Sustain. Chem. Eng. 1 (2013) 591–602.
[2] K.S. Prasad, P. Gandhi, K. Selvaraj, Synthesis of green nano iron particles (GnIP) and their application in adsorptive removal of as (III) and As(V) from aqueous solution, Appl. Surf. Sci. 317 (2014) 1052–1059.
[3] A. Ali, H. Zafar, Md. Zia, H. Ihsan ul, P. Abdul Rehman, J. Sarfraz Ali, H. Altaf, Synthesis, characterization, applications, and challenges of iron oxide nanoparticles, Nanotechnol. Sci. Appl. 9 (2016) 49–67.
[4] W. Wu, Q. He, C. Jiang, Magnetic iron oxide nanoparticles: synthesis and surface functionalization strategies, Nanoscale Res. Lett. 3 (2008) 397–415.
[5] S. Amyn, K. Pei-Yoong, Synthesis, properties, and applications of magnetic iron oxide nanoparticles, Prog. Cryst. Growth Charact. Mater. 55 (2009) 22–45.
[6] K. Kebede, A.M. KefeniTitus, T.I. Msagati Thabo, N. Bhekie, B. Mamba, Synthesis and application of hematite nanoparticles for acid mine drainage treatment, J. Environ. Chem. Eng. 6 (2018) 1865–1874.
[7] C. Wu, P. Yin, X. Zhu, Y. Chuanzi Ou, Y. Xie, Synthesis of hematite (α-Fe_2O_3) Nanorods: diameter-size and shape effects on their applications in magnetism, lithium ion battery, and gas sensors, J. Phys. Chem. B 110 (2006) 17806–17812.
[8] N. Hasan, Z. Guo, H.F. Wu, Biofabrication of Fe nanoparticles in aqueous extract of *Hibiscus sabdariffa*with enhanced photocatalytic activities, Anal. Bioanal. Chem. 408 (2016) 6269–6281.
[9] S. Naz, M. Islam, S. Tabassum, N.F. Fernandes, E.J.C. Blanco, M. Zia, Green synthesis of hematite (α-Fe2O3) $_n$a$_n$oparticles using Rhus *punjabensis extra*ct and their biomedical prospect in pathogenic diseases and cancer, J. Mol. Struct. 1185 (2019) 1–7.
[10] L.K. Ruddaraju, S.V.N. Pammi, G.S. Guntuku, V.S. Padavala, V.R.M. Kolapalli, A review on anti-bacterials to combat resistance: from ancient era of plants and metals to present and future perspectives of green nano technological combinations, Asian J. Pharm. Sci. (2019) in press.
[11] P.P.N. Vijay Kumar, U. Shameem, R.L. Kalyani, S.V.N. Pammi, Ultra small, monodispersed green synthesized silver nanoparticles using aqueous extract of *Sida cordifolia* plant and investigation of antibacterial activity, Microb. Pathog. 124 (2018) 63–69.
[12] N.P.S. Acharyulu, P. Madhu Kiran, K. Pratap, R.L. Kalyani, S.V.N. Pammi, Room temperature synthesis and evaluation of antibacterial activity of silver nanoparticles using Phyllanthus amarus leaf extract, J. Bionanoscience 8 (2014) 190–194.
[13] R.L. Kalyani, S.V.N. Pammi, P.P.N. Vijay Kumar, V.S. Padavala, K.V.R. Murthy, Antibiotic potentiation and anti-cancer competence through bio mediated ZnO nanoparticles, Mater. Sci. Eng. C 103 (2019) 109756.
[14] P.P.N.V. Kumar, U. Shameem, R.L. Kalyani, P. Kollu, S. Khan, S.V.N. Pammi, Antibacterial activity assessment and characterization of green synthesized CuO nano rods using *Asparagus racemosus* roots extract, SN Appl. Sci. 1 (2019) 421.
[15] G. Silvia, S. Raja, T. Varadavenkatesan, V. Ramesh, Structural characterization, antibacterial and catalytic effect of iron oxide nanoparticles synthesised using the leaf extract of Cynometra ramiflora, J. Mol. Struct. 1128 (2017) 572–578.
[16] B. Shahana, A. Kumar, S. Raja, Facile synthesis of magnetic iron oxide nanoparticles using inedible *Cynometra ramiflora* fruit extract waste and their photocatalytic degradation of methylene blue dye, Mater. Res. Bull. 97 (2018) 121–127.
[17] M.-C. María, L.-C. Marta, J.L. Barriada, H. Roberto, E. Manuel, de V. Sastre, Green synthesis of iron oxide nanoparticles. Development of magnetic hybrid materials for efficient as (V) removal, Chem. Eng. J. 301 (2016) 83–91.
[18] C.P. Devatha, T. Arun Kumar, K. Swetha, Green synthesis of Iron Nanoparticles using different leaf extracts for treatment of domestic wastewater, J. Clean. Prod. 139 (2016) 1425–1435.
[19] Y. Yen Pin, K. Shameli, M. Miyake, A. Khairudin, M. Shaza Eva Bt, T. Naiki, K. Xin, Green biosynthesis of superparamagnetic magnetite Fe3O4 nanoparticles and biomedical applications in targeted anticancer drug delivery system: a review, Arab. J. Chem. (2018) in press.
[20] A.A. Khaleel, Nanostructured Pure c-Fe2O3 via forced precipitation in an organic solvent, Chem. Eur J. 10 (2004) 925–932.
[21] A. Galal, V. Raman, I.A. Khan, *Sida cordifolia*, a traditional herb in modern perspective – a review, Curr. Trad. Med. 1 (2015) 5–17.
[22] L. Wan, S. Yan, X. Wang, Z. Li, Z. Zou, Solvothermal synthesis of monodisperse iron oxides with various morphologies and their applications in removal of Cr(VI), Crystallogr. Eng. Commun. 13 (2011) 2727.
[23] A. Rufus, N. Sreeju, D. Philip, Synthesis of biogenic hematite (α-Fe_2O_3) nanoparticles for antibacterial and nanofluid applications, RSC Adv. 6 (2016) 94206–94217.
[24] M. Bhushan, S. Muthukamalam, S. Sudharani, K.V. Annamraju, Synthesis of α-$Fe_{2-x}Ag_xO_3$ nanocrystals and study of their optical, magnetic and antibacterial properties, RSC Adv. 5 (2015) 32006–32014.